**Supporting Information**

# In-situ Generated Hydrophobic Micro Ripples via p-p Stacked Pop-up Reduced Graphene Oxide Nanoflakes for Extended Critical Heat Flux and Thermal Conductivities

**Ravi Kumar Cheedarala[1]*, and Jung Il Song[1]***

[1]Department of Mechanical Engineering, Changwon National University, Changwon, 51140, Republic of Korea.

## 1.0. Mechanism of Pool boiling CHF on the wire surface

Mechanism and Effect of Pop-rGO-Nf on CHF compared with DI water: The pbCHF shows the dynamic effervescing phenomenon through the phase transformation from a liquid to vapor during heat transfer because of the distribution of the excess thermal energy from the deposited Pop-rGO wire surface [1]. In general, the convection process is playing a high influence on the heat transfer mechanism, initially, which shows relatively low heating rate. As soon as the heat flow of the wire surface is reached to saturation point, the isolated bubbles were started generating from the nucleation sites of deposited Pop-rGO-Nf, Figure S1a. The generated water vapor bubbles size is increased by acquiring the vapor gently Figure. S1b-c. As the heat flux gradually upsurges, the size of water vapor bubbles was gradually increased through the interaction with the wire surface and amalgamation to obtain successive secondary bubbles which can metamorphosis into mushroom models. With increasing the superheat, more nucleation sites generated through vapor proliferates and ultimately forms vapor blanket at the interface (Figure. S1 d-e). The rapid bubble formation was inhibited from the cooling liquid when CHF is in progress the sudden rise in temperature occurs and started the nucleate pool boing rapidly which allows growing surface temperature. The CHF is strongly dependent on the heater geometry, flow conditions, gravity, and system pressure (Figure.S1f) [2-4]. Previous studies reveal that the CHF may enhance due to formation of scratching of the surface or by introducing surface-active agents and surfactants. But in our case, Pop-rGO-Nf concentration increases, simultaneously, the wire heat resistance also increased. Surprisingly, this increase was not related to an increase in nucleate density, because the size of the departing bubbles increased in the presence of the Pop-rGOs, and the bubble departure frequency decreased significantly [5]. This lack of improvement in the heat transfer coefficient also indicates that the observed behavior cannot be directly correlated with an increase in the TC of the Pop-rGO-Nf. However, Pop-rGO-Nf deposition has noted that the presence of Pop-rGOs decreased the number of active

nucleation sites on the heater surface. A significant decrease in bubble size and an increase in departure frequency suggest enhanced nucleation density, due to the increase in surface wettability [6]. The physical mechanism responsible for this discrepancy remains unclear and highlights the significant inconsistencies present in the field. One potential explanation is that the Pop-rGOs behave as nucleation sites for bubble growth, but exhibit stronger interactions with the bubble, due to their curvature and irregular shape (particularly if in the fractal configuration). This would result in greater coalescence among individual bubbles at a lower super-heat and may account for the observed behavior were shown in Figure S1. In our previous studies, for extended CHF we used CuO-CS nano templates and produced similar evolution of vapor bubbles and transformed into vapor bubbles jacket during CHF experiment [1]. At the present, we observed similar kind of trend using Pop-rGO-Nf which is strongly suggested our hypothetic mechanism for extended CHF values.

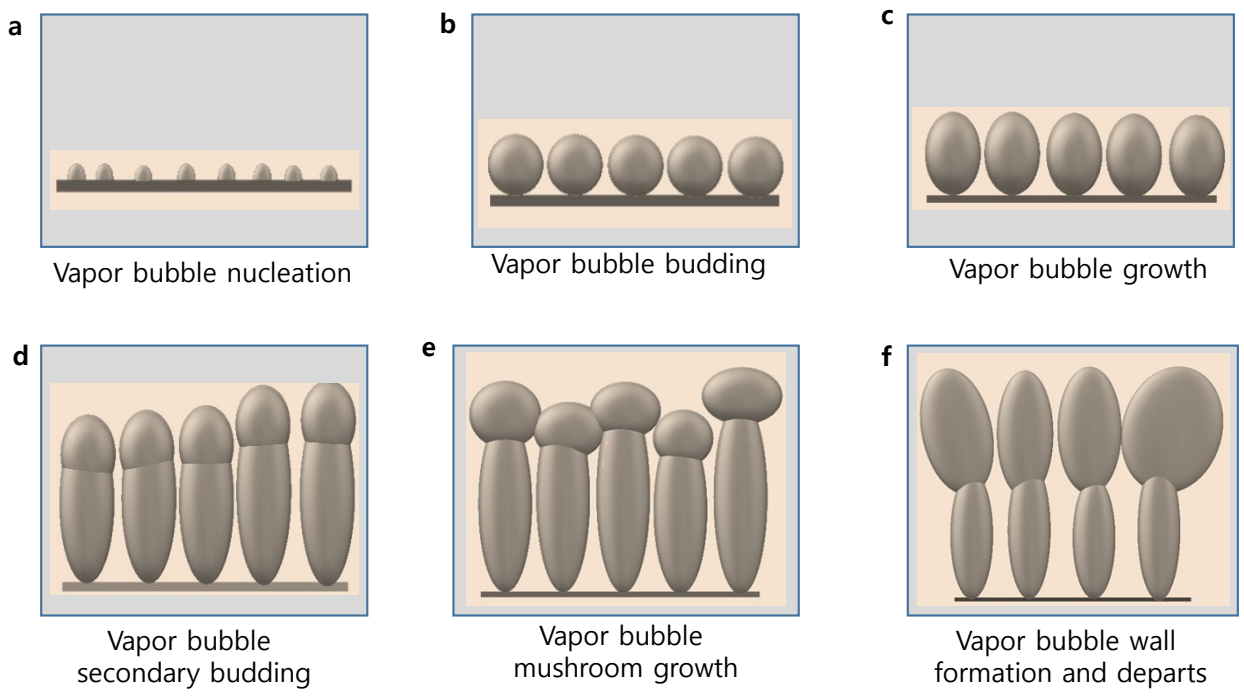


**S1**. (a–f). Evolution of bubble nucleation growth from a 500 μm-diameter NiCr wire surface coated with 0.01-wt% Pop-rGO-Nf, under a heat flux of 1095 kW/m$^2$.

## 2. Confirmation of the Pop-rGO-micro ripples

We investigated the magnified FE-SEM images that showed the morphology of micro-rippled structures on the wire surface, **S2** showed the micro-rippled structures comprised of heights and valleys with nano-scale cavities. The nano-scale cavities can provide capillarity to facilitate continuous vapor formation from the wire surface, while the large pores maintain a high permeability, which allows both penetration of liquid into the pores of the developed rGO film and the escape of vapor bubbles from the Pop-rGO ripples. Therefore, the porous structure of the rGO rippled structures improves the migration of the departing vapor bubbles and the liquid hinders the development of a vapor blanket, which could degrade both CHF and HTC, inside the porous structure of the Pop-rGO channels. Figure. S2a and S1b, shown the height, width and channel of the Pop-rGO by π-π stacking's were from ~5.6 to 7.2 m, ~2.6 m and 2.05 m, respectively. The regular nanopores (Figure. S2c) and channels (Figure. S2d) were found on the rGO rippled structures due to π-π stacking's at basal planes of Pop-rGO nanosheets and chelation of adjacent carboxylic acid functional groups of individual Pop-rGO sheets through the formation of hydrogen bonding. The inset red color circle and bars were clearly evidenced in Figure. S2d for supporting our investigation. These nano-cavities were strongly facilitated to the evolution of water bubbles while heating of wire during CHF experiment. In addition, the hydrophobicity was also increased with an increase of roughness on the wire surface by an increase of deposition of Pop-rGO nanosheets as a layer-on-layer network.

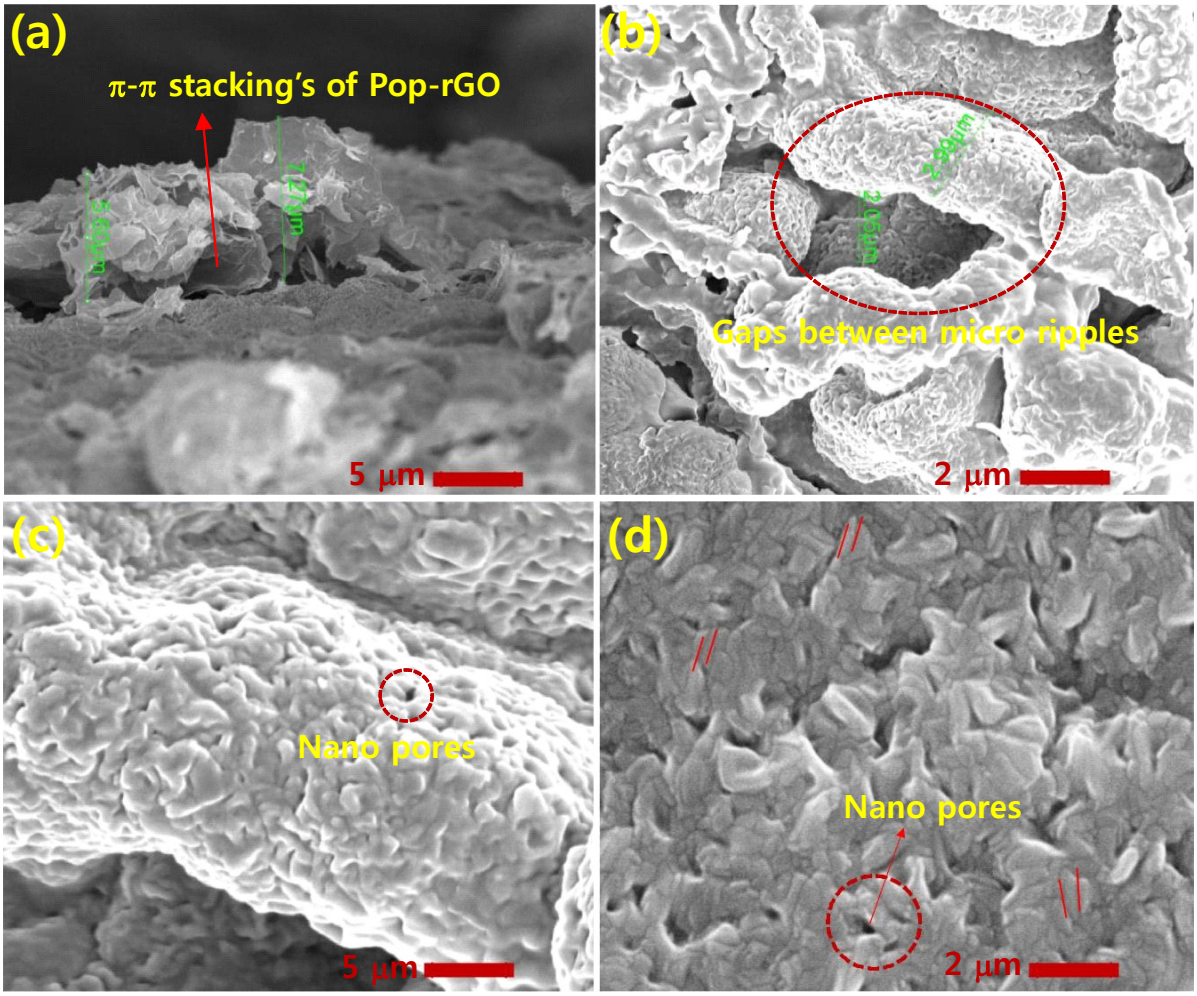


**S. 2**. Magnified FE-SEM images of micro rippled structures on the built-up wire surface, a) **π-π** stacking's of Pop-rGO with the height of ~7.27 μm; b) the width and gap of Pop-rGO-ripples ~3 μm ~2 μm and; c) Nano pores were shown on the ripples; d) Nano pores and with carboxylate bridges between Pop-rGO layers were appeared on the magnified image (inset, red circle and bars).

## 3. Experimental

### 3.1. Preparation of few-layered GO [18]

GO was prepared from natural graphite by the well-known Hummers method with minor modifications. In brief, 2 g of natural graphite powder was added to a 250-mL beaker, and then 1 g of $NaNO_3$ and 46 mL of $H_2SO_4$ were sequentially added while stirring in an ice-bath. Next, 6 g of $KMnO_4$ was slowly added to the beaker while stirring and the temperature was maintained below 20 °C. The ice-bath was removed after 5 min and the reaction mixture was maintained at

35 °C for 30 min, and then 92 mL of water was slowly added to the reaction mixture. The mixture was then stirred for another 15 min. Next, 80 mL of hot water and 30% $H_2O_2$ aqueous solution were added at 60 °C to reduce the residual $KMnO_4$ and stirred until no bubbles were present. Finally, the reaction mixture was centrifuged at 8000 rpm for 30 min, the supernatant was discarded and the obtained powder was washed by warm water until the pH reached to 7. The obtained yellow-brown powder was re-dispersed in ultrapure water and sonicated for 30 min. Homogeneous suspensions of various concentrations were formed after filtering to remove the trace black residues. GO powder was obtained after drying the suspensions at 60 °C.

**3.2. Preparation of Chemically reduced graphene oxide (C-rGO) [19].**

According to the literature method with little modification, the chemically-reduced graphene oxide (rGO) were also synthesized by a classically modified hydrazine hydrate chemical reduction method. 0.6 ml of hydrazine hydrate was to the colloidal dispersion of 100 mg of GO in 20 ml of DI water and the solution was heated at 90 $^oC$ for 12 h under magnetic stirring. The reaction mixture was cooled to room temperature, decanted the separated water, and washed with absolute alcohol at least 6 times by centrifuging, re-dispersing and dried to obtain C-rGO.

**References**

[1]. R. K. Cheedarala, E. Park, K. Kong, Y. B. Park, H. W. Park, Experimental study on critical heat flux of highly efficient soft hydrophilic CuO–chitosan nanofluid templates, *Int. J. Heat and Mass Transf.* 2016, *100*, 396-406.

[2]. C. C. Chusuei, M. A. Brookshire, D. W. Goodman, Correlation of relative X-ray photoelectron spectroscopy shake-up intensity with CuO particle size, *Langmuir,* 15 (1999), pp. 2806-2808.

[3]. C. Huo, J. Ouyang, H. Yang, CuO nanoparticles encapsulated inside Al-MCM-41 mesoporous materials via direct synthetic route, *Sci. Rep.,* 4 (2014), p. 3682.

[4]. S. G. Kandlikar, Heat transfer mechanisms during flow boiling in microchannels, *J. Heat Transfer,* 126 (1) (2004), pp. 8-16.

[5]. G. Hetsroni, A. Mosyak, Z. Segal, G. Ziskind, A uniform temperature heat sink for cooling of electronic devices, *Int. J. Heat and Mass Transfer*, 45 (2002), pp. 3275-3286.

[6]. S. M. You, J. H. Kim, K. H. Kim Effect of nanoparticles on critical heat flux of water in pool boiling heat transfer, *Appl. Phys. Lett.,* 83 (2003), pp. 3374-3376.